Jestr

Journal of Engineering Science and Technology Review 17 (4) (2024) 16-22

Research Article

JOURNAL OF
Engineering Science and Technology Review

www.jestr.org

Investigation on the Role of Interface on Electrical, Thermal and Mechanical Properties of Silicone Rubber-BN Nanocomposites

K. Ganesan[1], Manoj Dhivakar J.[1], Stefan Kornhuber[2], Ramanujam Sarathi[1] and M. G. Danikas[3,*]

[1]*Department of Electrical Engineering, IIT Madras, Chennai 600036 – India*
[2]*Department for High Voltage Engineering, University of Applied Sciences, Zittau/Görlitz 02763 - Zittau Germany*
[3]*Department of Electrical & Computer Engineering, Democritus University of Thrace (DUTh) Xanthi, Greece*

Received 2 April 2024; Accepted 14 July 2024

Abstract

The current study investigates the impact of interfacial interactions between the silicone rubber base polymer matrix and the hexagonal boron nitride (hBN) nanofiller, incorporated at different weight percentages, on electrical, thermal, and mechanical properties. The adhesion of filler to the polymer is examined through swelling tests and Kraus plots and the elastic modulus calculated has a good agreement with the experimental data. The addition of 3 wt% of BN nanofiller with silicone rubber led to a 25.4 % increment in surface discharge inception voltage (SDIV). The Thermogravimetric analysis (TGA) shows that the BN filler included samples have high degradation temperature and thermal activation energy. The introduction of filler into the base polymer matrix significantly enhances mechanical properties, specifically tensile strength, tensile modulus, and percentage elongation at break.

Keywords: Silicone Rubber, Boron nitride, Surface discharge, TGA, Mechanical tests.

1. Introduction

Polymer insulators are attracting more attention in AC and DC power system insulation structures because of their lightweight, easy transportation, and superior performance when compared to their ceramic counterparts[1]. In addition, they possess excellent electrical, mechanical, and thermal properties, good hydrophobicity, and vandalism resistance[2].Many researchers have shown that the addition of a small amount of fillers to the base polymer improves tracking and erosion performance, corona aging resistance, and pollution performance[3]. The dielectric properties of silicone rubber incorporated with various nanofillers such as Silica, Alumina, and ATH are improved when compared to that of pristine silicone rubber[4][5]. Hexagonal boron nitride (h-BN) nanoparticles hold promise as a material due to their exceptional dielectric properties, boasting a lower relative permittivity compared to other ceramic fillers such as Al_2O_3 and AlN [1]. They exhibit high thermal conductivity (200–300 W/m. K), compared to AlN (150 W/m. K), Al_2O_3 (38.42 W/m. K), Si_3N_4 (86.120 W/m. K), SiC (85 W/m. K), ZnO (60 W/m. K) etc. Since, thermal conductivity plays a major role in tracking and erosion of the material, BN filler could improve the tracking resistance of the silicone rubber material [8]. BN materials possess impressive mechanical strength akin to graphene (h-BN is also referred to as white graphene), and demonstrate high thermal and chemical stability alongside good biocompatibility [2]. Studies have demonstrated that incorporating BN filler loadings of up to 32 wt% enhances the thermal conductivity of silicone rubber composites by approximately 30%. It was also reported that the addition of small amount of BN filler improves the vulcanization behaviour and breakdown strength of the silicone rubber when compared to other fillers [9].

Hexagonally structured boron nitride (hBN) nanofiller has a crystal structure similar to that of carbon and possesses high thermal conductivity and mechanical properties when compared to that of other nanofillers. Zhu et al have shown the effect of crosslinking density on zirconia-added silicone rubber composites to have high bond strength but further analysis with cross-linking density and filler-polymer interaction has to be carried out for boron nitride filled composites[10]. Khanum et al have studied the thermal properties of silicone rubber composites with hBN and concluded that it has good heat transport properties[11]. Du et al have shown that the silicone rubber filled with boron nitride nanofiller has got superior resistance to tracking and erosion under DC voltages[12]. Zhou et al have shown BN added XLPE has enhanced dielectric properties[13].The interface between the polymer and the nanoparticle plays a significant role in determining the desirous properties of the composite. The interface between the boron nitride nano filler ad the base polymer matrix (Polydimethylsiloxane) has to be investigated for understanding the improvement in the electrical, thermal and mechanical performance of the nanocomposites as much of the work was not carried out in understanding the interface between the filler and base polymer matrix. Thermogravimetric analysis is widely used for understanding the thermal degradation and thermal stability and even oxidation behaviour of the polymer composites. Zhao.et.al studied the thermal degradation kinetics of silicone rubber filled with ceramifiable fillers and calculated the activation energy for the composites[14].

The investigation of the mechanical properties of the nanocomposites were carried out by many researchers. Shahamatifard.et.al has carried out the thermal and mechanical analysis of carbon nanotube based silicone rubber composites and concluded that incorporating small amount of carbon in to the base resin greatly enhances the mechanical properties of the matrix[15] but the reason behind

*E-mail address: mdanikas@ee.duth.gr
ISSN: 1791-2377
doi:10.25103/jestr.174.03

this has to be analysed. High thermal conductivity of a basic polymer can be achieved by forming a network of highly conducting fillers within the polymer matrix, which requires high filler loadings. This leads to a rise in viscosity, which lowers the quality of the moulded product. Even with modest filler loadings, inorganic fillers with large aspect ratios, like BN, create a more efficient thermal conductive network than fillers with low aspect ratios [16]. On the other hand, significant nanofiller loading might result in a decrease in thermal conductivity values by increasing filler–polymer contacts. However, the thermal conductivity of the entire polymer material might be greatly improved by adding a smaller ratio of highly thermally conductive BN filler, which would result in a cost-efficient method for commercial applications.

On understanding the above points, the present study focuses on (i) the understanding of DC surface discharge characteristics with different concentrations of BN-added silicone rubber nanocomposites, (ii) The interface interaction between filler and base polymer through equilibrium swelling test and Kraus plots the cross-linking density calculation of silicone rubber/BN composites and the correlation with the elastic modulus, (iii) the investigation of the thermal stability and degradation analysis using TGA. (iv) Tensile strength, Tensile modulus or elastic modulus and percentage elongation at break are analysed through Universal mechanical strength tests.

2. Experimental Studies

Sample preparation

Nanocomposites of silicone rubber are produced utilizing boron nitride (BN) nanoparticles, possessing an average diameter of 100 nm and a purity of 99.9% sourced from Hongwu Nanometer in China. To eliminate moisture content from the nanoparticles, they undergo oven-drying for a duration of 24 hours at 150°C. Subsequently, the dried nanoparticles are weighed to achieve the desired weight percentage for the silicone rubber. They are then dispersed in ethyl alcohol using a shear mixer and subjected to sonication for 30 minutes in an ultrasonicator. The sonication is conducted in pulse mode, alternating between a 9-minute on and off period, ensuring thorough dispersion of the nanoparticles. The solution containing boron nitride and ethyl alcohol is then mixed with polydimethylsiloxane (RTV8112 Momentive, USA) and subjected to shearing for 30 minutes. A curing agent (Hardener RTV 9858) is added in a 1:10 ratio using a shear mixer and promptly degassed under vacuum to remove any moisture from the mixture. To ensure proper solidification of the nanocomposite, the blend is poured into a 100 mm x 100 mm x 3 mm mold and compressed at room temperature under 0.1 MPa for 24 hours. Silicon rubber nanocomposites are formulated with varying weight percentages (0, 1, 3, or 5) of boron nitride filler. Samples are labelled accordingly (S0, S1, S3, and S5) based on the percentage of nanofillers used. The steps involved in the sample preparation is illustrated in the Fig.1.

Cross-Linking Density

The equilibrium swelling method is used for calculating the cross-linking density. The initial weight of the silicone rubber was measured using a weigh balance machine with an accuracy of ± 0.1 mg at 25 ºC and it is taken as m_0. Then the sample is immersed in 25 ml of toluene for 24 hours to obtain swelling equilibrium. The swelling weight m_s was measured after the sample was taken out from the toluene and wiped with the tissue. The cross-linking density (D) and the average molecular weight per vulcanization point (M_c) were calculated by using the Flory-Rehner equation [17].

$$\varphi = \frac{\frac{m_0}{\rho}}{\frac{m_0}{\rho}+\frac{m_s-m_0}{\rho_c}} \quad (1)$$

$$M_c = -\frac{\rho\, V_0 \varphi^{1/3}}{\ln(1-\varphi)+\varphi+\psi\varphi^2} \quad (2)$$

$$D = \frac{1}{2M_C} \quad (3)$$

where φ is the volume fraction of the silicone rubber in the swelled sample. m_0 and m_s are the weights of the silicone rubber sample before and after immersing it in the toluene solvent. ρ and ρ_c are the density of the silicone rubber and toluene respectively. V_0 is the molar volume of the toluene (106.54 x10^{-3} L/mol), M_c is the average molecular weight per vulcanization point (g/mol), D is the crosslinking density (mol/g) and ψ is the interaction parameter between silicone rubber and toluene which is taken as 0.456[17]. The volume fraction is calculated from the weight fraction using equation (4).

$$\Phi = \frac{W}{W+(1-W)\frac{\rho_f}{\rho_m}} \quad (4)$$

Where W is the weight fraction of the filler, ρ_f, *and* ρ_m are the densities of the filler and polymer matrix respectively.

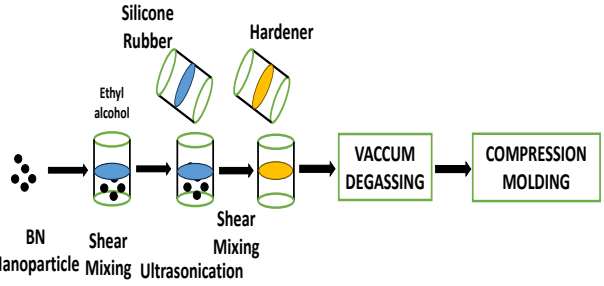

Fig. 1. Sample Preparation

DC Surface Discharge Studies

A 100 kV, 5 kVA, transformer was connected to a voltage doubler circuit to generate the required DC voltage. All the studies were restricted only to positive DC voltage. The experimental setup for DC surface discharge studies is shown in Fig. 2. The IEC (B) electrode according to IEC60270 was used as a high voltage electrode and an aluminium circular electrode with a thickness of 15 mm and a diameter of 50 mm was considered as a ground electrode. The sample with a size of 2 cm × 2 cm and a thickness of 2 mm was placed between the electrodes and the rate of raise of voltage was maintained at 500 V/s. In this study, an Ultra-High Frequency (UHF) sensor was positioned 20 cm away from the electrode arrangement, and discharge signals were captured using a digital storage oscilloscope (specifically, a LeCroy four-channel digital real-time oscilloscope) with a bandwidth of 3 GHz and a sampling rate of 20 GSa/s. The voltage corresponding to the first detected UHF signal was recorded, and the average of ten readings was taken as the surface discharge voltage for analysis.

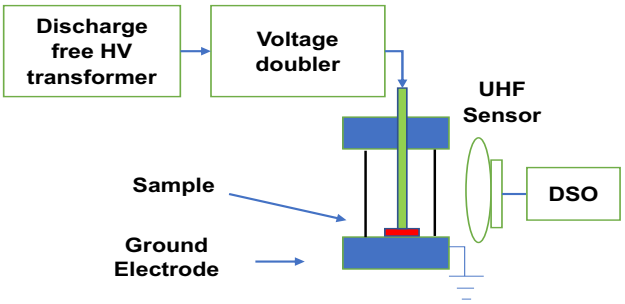

Fig. 2. Experimental setup for surface Discharge inception voltage measurement.

Thermogravimetric Analysis (TGA)

The thermal stability and degradation dynamics of silicone rubber composites were investigated using thermogravimetric analysis. The thermogravimetric analysis of the materials was performed using a Labsys evo TGA apparatus from Setaram Instruments, France. 30 mg of each unfilled and composite sample was utilized, and the temperature range was set at 30 ºC to 750 ºC with a heating rate of 20 ºC/min at argon atmosphere.

Mechanical Tests

The Tensile Strength, Tensile modulus and the percentage elongation at break are measured using Instron 5kN Ultimate tensile strength tester from Germany with a displacement rate of 250mm/min at room temperature. The samples are specifically prepared in dumbbell shape for these tests with dimensions of 115mm X 6mm X 3mm with a gauge length of 25mm as per ASTDM D412 standards as shown in Fig.3. Each sample is tested for three times and the average value is plotted.

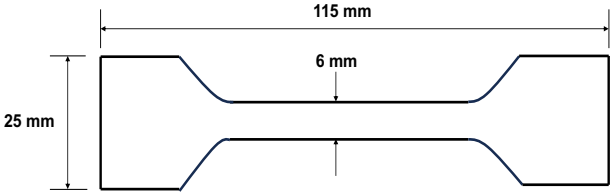

Fig. 3. Sample shape for Mechanical Tests.

3. Results and Discussions

Cross-Linking Density

Figure 4. shows the cross-linking density of silicone rubber composites calculated using (5). The cross-linking density is observed to be higher for composite samples compared to the virgin silicone rubber sample. It is noticed that the 5wt % of BN filler added to sample S5 shows a 40 % increase in the cross-linking density. The high cross-linking density value indicates the formation of strong covalent bonds between the main chain (Si-O-Si) and the side chain (-CH_3) in the composite samples[18]. The increase in the cross-linking density also restricts the movement of the rubber molecules and hence provides a stable chemical resistance property [19]. Du et al [20] indicated that the average molecular weight per vulcanization point and the cross-linking density is directly related to the elastic modulus which is given by

$$E = \frac{3\rho RT}{M_c} \tag{5}$$

where E is the elastic modulus, ρ is the density of the silicone rubber, R is the universal gas constant, T is the ambient temperature and M_c is the average molecular weight per vulcanization point (g/mol). Since the elastic modulus has a direct relation with the cross-linking density the average molecular weight per vulcanization point is observed to be inversely proportional to the cross-linking density. Therefore, an increase in the cross-linking density could also result in high elastic modulus values as shown in Fig. 4. The higher values of elastic modulus are attributed to the increase in the strength of deformation. The increase in elastic modulus directly conveys that the composite sample provides stable strength against surface discharges and tree formation as a greater number of bonds needs to be broken in filler-added samples [20].

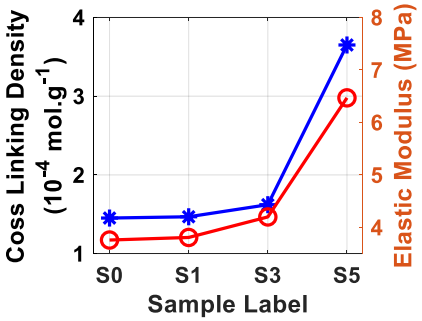

Fig. 4. Variation in Cross-linking density and elastic modulus of silicone rubber-BN nanocomposites.

The polymer-filler interaction and their interfacial area play a vital role in determining the characteristics of composites. The increase in the interfacial area is attributed to adsorbing more polymer chains to the filler surface which provides the desired mechanical and thermal performance[21]. The polymer-filler interaction can be well understood by the swelling tests and Kraus plot. The Kraus plot demonstrates the theory of polymer-filler interaction through a theory that reports that the swelling of the polymers in some solvents like toluene, and benzene obeys the following equation[22].

$$\frac{D_f}{D_0} = 1 - m\left(\frac{\Phi}{1-\Phi}\right) \tag{6}$$

$$m = 3c\left(1 - v_{f0}^{\frac{1}{3}}\right) + v_{f0} - 1 \tag{7}$$

Where D_f and D_0 are the cross-linking density of filled and unfilled composites which can be calculated using (3), Φ is the volume fraction of the filler. c is the characteristics of the filler which does not depend on the solvent nature and type of base polymer. Equation (6) is of the form of straight-line characteristics $y = mx + c$ where c is the intercept which is approximately equal to one and m is the slope of the line. If we plot the ratio $\frac{D_f}{D_0}$ vs $\left(\frac{\Phi}{1-\Phi}\right)$, we should get a line with a negative slope.

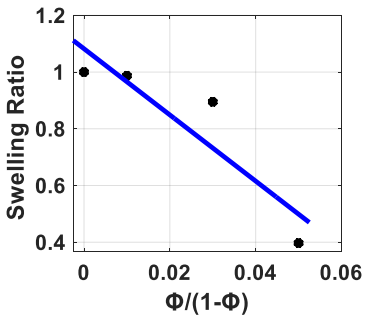

Fig. 5. Kraus plot of SR-BN composites.

Fig 5. Shows the Kraus plot for SR nanocomposites after fitting the data with a linear fit and it can be seen that the slope for S1 is approximately 0.98 whereas for S5 it is 0.4. According to Kraus's theory, the reduction in the swelling ratio is an indication of better filler-polymer interaction, and thus the adsorption of the filler to the polymer chain is greatly enhanced thereby increasing the interfacial area which in turn increases the mechanical strength of the composites[23].

Surface Discharge Inception Voltage (SDIV)

The variation in surface discharge inception voltage (SDIV) of SiR-BN nanocomposites is shown in Fig. 6. The 3 wt% of BN filler added nanocomposite samples shows a 25.4 % increase in SDIV values compared to the virgin sample. The further increase in the filler concentration resulted in lower SDIV values. The reduction in the SDIV as the filler concentration increased can be attributed to several factors. The agglomeration formation at higher concentrations of fillers resulted in early surface discharges[24]. Zhang et al indicated that the DC surface flashover voltage of SiR/hBN nanocomposites not only depends on the interaction between the filler and polymer matrix but also the orientation of the filler with respect to the electrode arrangement. The orientation of the filler greatly influences the carrier mobility. It is also indicated that the out-of-plane orientation has higher carrier mobility compared to the in-plane orientation hence increasing charge transportation inside the samples [25]. The charge traps created by the addition of nanofiller have a greater influence on the surface discharge inception voltage.

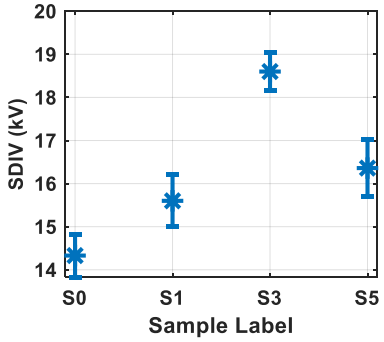

Fig. 6. SDIV Variation of SR-BN nanocomposites.

Thermogravimetric Analysis

The TG and DTG curves for the virgin and nanocomposites are shown in Fig. 7a and 7b respectively. From Fig. 7a, it is noticed that the initial degradation of the silicone rubber samples S1, S3, and S5 started at 360 ºC, 395 ºC, 420 ºC, and 454 ºC, respectively. The addition of BN filler with base silicone rubber significantly increases the initial degradation temperature. A marginal variation in percentage weight reduction is observed with 5 wt% filler added to sample S5. From the DTG curves shown in Fig. 7b, a marginal variation in maximum degradation temperature is observed with the virgin and composite samples. The rate of degradation at maximum temperature is noticed as 1.98 mg/ ºC, 0.75 mg/ ºC, 0.62 mg/ ºC, and 1.12 mg/ ºC for the samples S0, S1, S3, and S5, respectively. However, the virgin silicone rubber S0 shows a significantly high rate of degradation at maximum temperature compared to filler samples. This indicates the thermal stability of silicone rubber samples with the addition of BN fillers. TGA (Thermogravimetric Analysis) and DTG (Derivative Thermogravimetric) curves provide valuable data for determining the thermal activation energy (Ea), which represents the minimum energy necessary to trigger thermal degradation. The activation energy was calculated using the method proposed by Horowitz and Metzger [26], [27]

$$\ln\left\{ln\left[\frac{W_0-W_f}{W-W_f}\right]\right\} = \left(\frac{E_a}{RT^2}\right)\theta \quad (8)$$

By considering, $\ln\left\{ln\left[\frac{W_0-W_f}{W-W_f}\right]\right\}$ = K, the equation (5) becomes

$$K = \left(\frac{E_a}{RT^2}\right)\theta \quad (9)$$

W_0 *and* W_f are the initial and final stage weights of the sample, and R is the universal gas constant. W represents the remaining weight at a specific temperature. The difference between the temperature T and T_s is taken as θ. T_s is the temperature at which the following equation holds true.

$$\left[\frac{W_0-W_f}{W-W_f}\right] = \frac{1}{e} = 0.3679 \quad (10)$$

Equation (9) is in the form of a straight-line equation as shown in Fig. 8, hence from the slope of the plot of K Vs θ, one can calculate thermal activation energy. The calculated values of the thermal activation energy E_a and T_s are shown in Table 1. It is noticed that the increase in filler concentration gradually increases the initial degradation temperature and thermal activation energy.

Table 1. Thermal Kinetic Parameters of Sr-Bn Nanocomposites

Sample Label	Activation Energy, Ea (kJ/mol)	Temperature, Ts (ºC)
S0	21.62	406.08
S1	22.14	410.43
S3	24.43	418.56
S5	27.02	429.13

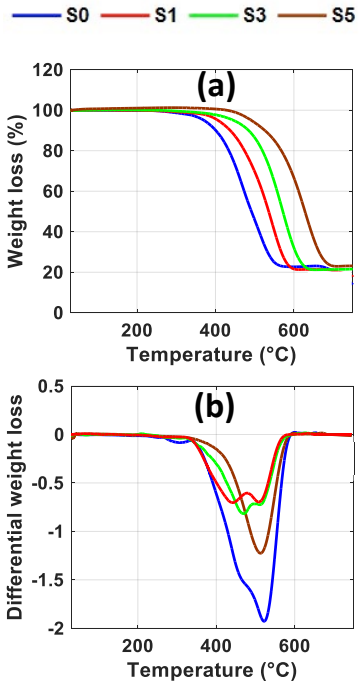

Fig. 7. Changes in thermogravimetric curves of SR-BN nanocomposites. a) TG curves b) DTG curves

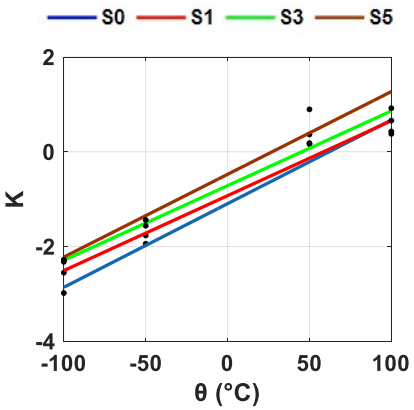

Fig. 8. K Vs θ plots of SR-BN nanocomposites.

Mechanical Tests

The stress-strain curves for silicone rubber and composites are shown in Fig.9. Silicone rubber has a linear stress-strain relationship. When the silicone rubber is stretched, it leads to the opening of the kinks hence larger strain is obtained by applying little stress. Prolonged stretching leads to the polymer chains getting aligned which in turn causes the crystallinity to increase and hence the stress[28].

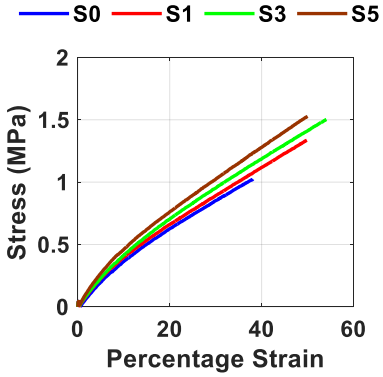

Fig. 9. Stress-Strain curves of SR-BN nanocomposites.

The tensile strength of the pristine and composites are shown in Fig.10.The tensile strength of S5 increases to 125% when compared to that of the S0 sample. The tensile strength of the silicone rubber composites increases with increase in the filler concentration due to the better interface interaction between the base polymer and the nanoparticle. The increase in the tensile strength causes the load to be transferred from polymer chain to the nanoparticle.

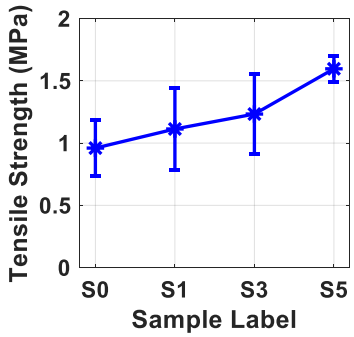

Fig. 10. Tensile strength of SR-BN nanocomposites.

The boron nitride nano particle has large surface area hence it can absorb more load from the polymer chains this causes the tensile strength to increase as the filler concentration increases which is also obvious from the standard deviation getting reduced. Pukanzsky.et.al developed an empirical model relating the debonding stress and size of the particle which is given by[29]

$$\sigma^D = -C_1\sigma^T + [\left(\frac{C_2 W_{mf}}{R}\right)]^{0.5} \quad (11)$$

Where, σ^D and σ^T are the debonding and thermal stress. C_1 and C_2 are the constants, R is the radius of the nanoparticle. W_{mf} is the work of adhesion. It can be seen that the radius of the nanoparticle is in inverse relation with the debonding stress.

The percentage elongation at break for silicone rubber composites are shown in Fig.11. The percentage elongation is increased to about 39% for S5 when compared to that of S0 this due to the fact that the elongation at break directly indicates the withstand capability of the polymer. It is obvious from the Fig 11 that the addition of the filler increases the withstand capability of the composites due to better filler - polymer and filler-filler interface achieved by homogenous dispersion of the filler into the base resin.

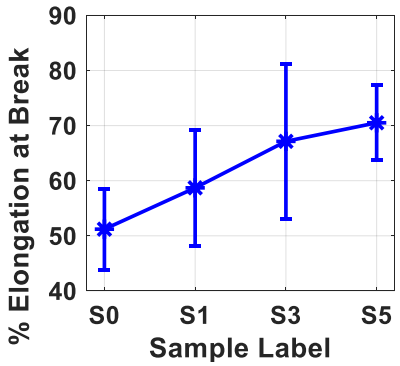

Fig. 11. Percentage elongation at break of SR-BN nanocomposites.

The variation of tensile modulus for silicone rubber composites is shown in Fig. 12. The tensile modulus follows a similar trend as tensile strength and elongation at break. The tensile modulus for S5 is increased to 38% when compared to S0. The addition of filler increases the cross-linking density of the composites which in turn causes a greater number of polymer chains to be broken as seen before Hence the tensile modulus is found to increase with the filler which is in good agreement with the elastic modulus calculated before.

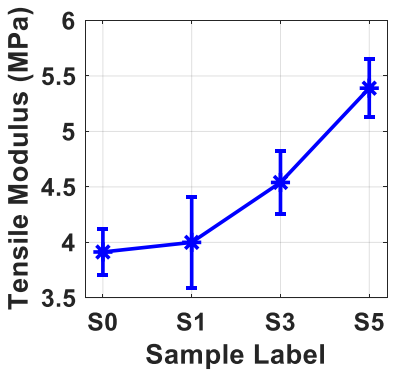

Fig. 12. Tensile modulus of SR-BN nanocomposites.

Also, methodical experimental studies need to be carried out with the nanocomposite material with different fillers, its performance as insulation structure under multi-stress condition to near condition compared with silicone rubber added hBN and the results will be reported in near future.

4. Conclusion

The major conclusions evolved from the present study are:

- The high cross-linking density and the elastic modulus with the inclusion of BN filler indicate the formation of strong covalent bonds which restricts the chain movement in silicone rubber matrix.
- The surface discharge inception voltage is improved with the addition of filler up to S3 and on further increase, the SDIV decreases.
- The TGA analysis shows improved thermal degradation kinetics and reduced weight loss upon the incorporation of fillers. The high activation energy of the composite samples denotes the high thermal stability of BN filler with silicone rubber matrix.
- In comparison to pristine silicone rubber, the filler added composites showed increased tensile strength about 125%, elongation at break about 39% and tensile modulus about 38%.

References

[1] E. A. Cherney, "50 years in the development of polymer suspension-type insulators," *IEEE Electr. Insul. Mag.*, vol. 29, no. 3, pp. 18–26, May 2013, doi: 10.1109/MEI.2013.6507410.

[2] T. Tanaka, G. C. Montanari, and R. Mulhaupt, "Polymer nanocomposites as dielectrics and electrical insulation-perspectives for processing technologies, material characterization and future applications," *IEEE Trans. Dielect. Electr. Insul.*, vol. 11, no. 5, pp. 763–784, Oct. 2004, doi: 10.1109/TDEI.2004.1349782.

[3] S. Jasmee, G. Omar, S. S. C. Othaman, N. A. Masripan, and H. A. Hamid, "Interface thermal resistance and thermal conductivity of polymer composites at different types, shapes, and sizes of fillers: A review," *Polymer Compos.*, vol. 42, no. 6, pp. 2629–2652, Jun. 2021, doi: 10.1002/pc.26029.

[4] E. A. Cherney, "Silicone rubber dielectrics modified by inorganic fillers for outdoor high voltage insulation applications," in *CEIDP '05. 2005 Ann. Rep. Conf. Electr. Insul. Dielect. Phenom., 2005*, Nashville, TN, USA: IEEE, 2005, pp. 1–9. doi: 10.1109/CEIDP.2005.1560607.

[5] S. Ilhan, D. Tuzun, and A. Ozdemir, "Comparative Properties of HTV Silicone Rubber for Composite Insulators—ATH and Silica Fillers," *IEEE Trans. Dielect. Electr. Insul.*, vol. 28, no. 2, pp. 414–422, Apr. 2021, doi: 10.1109/TDEI.2020.009183.

[6] Y. Jiang, X. Shi, Y. Feng, S. Li, X. Zhou, and X. Xie, "Enhanced thermal conductivity and ideal dielectric properties of epoxy composites containing polymer modified hexagonal boron nitride," *Compos. Part A: Appl. Sci. Manufact.*, vol. 107, pp. 657–664, Apr. 2018, doi: 10.1016/j.compositesa.2018.02.016.

[7] G. Sun, J. Bi, W. Wang, and J. Zhang, "Enhancing mechanical properties of fused silica composites by introducing well-dispersed boron nitride nanosheets," *Ceram. Int.*, vol. 44, no. 5, pp. 5002–5009, Apr. 2018, doi: 10.1016/j.ceramint.2017.12.096.

[8] S. Ansorge, F. Schmuck, and K. O. Papailiou, "Impact of different fillers and filler treatments on the erosion suppression mechanism of silicone rubber for use as outdoor insulation material," *IEEE Trans. Dielectr. Electr. Insul.*, vol. 22, no. 2, pp. 979–989, Apr. 2015, doi: 10.1109/TDEI.2014.004831.

[9] P. Liu, L. Li, L. Wang, T. Huang, Y. Yao, and W. Xu, "Effects of 2D boron nitride (BN) nanoplates filler on the thermal, electrical, mechanical and dielectric properties of high temperature vulcanized silicone rubber for composite insulators," *J. Alloys Compd.*, vol. 774, pp. 396–404, Feb. 2019, doi: 10.1016/j.jallcom.2018.10.002.

[10] X. Zhu, Y. Zhou, Y. Zhang, L. Zhou, and X. Huang, "The Effects of Nano-ZrO_2 on the Mechanical and Electrical Properties of Silicone Rubber and a Corresponding Mechanism Analysis," *IEEE Trans. Dielect. Electr. Insul.*, vol. 29, no. 6, pp. 2218–2226, Dec. 2022, doi: 10.1109/TDEI.2022.3203373.

[11] K. K. Khanum and S. H. Jayaram, "Improved Thermal Properties and Erosion Resistance of Silicone Composites With Hexagonal Boron Nitride," *IEEE Trans. on Ind. Applicat.*, vol. 58, no. 5, pp. 6583–6590, Sep. 2022, doi: 10.1109/TIA.2022.3186286.

[12] B. Du and H. Xu, "Effects of thermal conductivity on dc resistance to erosion of silicone rubber/BN nanocomposites," *IEEE Trans. Dielectr. Electr. Insul.*, vol. 21, no. 2, pp. 511–518, Apr. 2014, doi: 10.1109/TDEI.2013.004139.

[13] X. Zhou *et al.*, "Effect of Boron Nitride Concentration and Morphology on Dielectric and Breakdown Properties of Cross-Linked Polyethylene/Boron Nitride Nanocomposites," *Adv. Eng. Mater.*, vol. 23, no. 7, pp. 1–7, Jul. 2021, doi: 10.1002/adem.202100008.

[14] D. Zhao, T. Liu, Y. Xu, J. Zhang, Y. Shen, and T. Wang, "Investigation of the thermal degradation kinetics of ceramifiable silicone rubber-based composite," *J. Therm. Anal. Calorim.*, vol. 148, no. 13, pp. 6487–6499, Jul. 2023, doi: 10.1007/s10973-023-12138-9.

[15] F. Shahamatifard, D. Rodrigue, and F. Mighri, "Thermal and mechanical properties of carbon-based rubber nanocomposites: a review," *Plast. Rubber Compos.*, pp. 1–23, Oct. 2023, doi: 10.1080/14658011.2023.2231286.

[16] K. Ruan, H. Yan, S. Zhang, X. Shi, Y. Guo, and J. Gu, "In-situ fabrication of hetero-structured fillers to significantly enhance thermal conductivities of silicone rubber composite films," *Compos. Sci. Technol.*, vol. 210, Jul. 2021, doi: 10.1016/j.compscitech.2021.108799.

[17] P. J. Flory and J. Rehner, "Statistical mechanics of cross-linked polymer networks I. Rubberlike elasticity," *J. Chem. Phys.*, vol. 11, no. 11, pp. 512–520, Nov. 1943, doi: 10.1063/1.1723791.

[18] K. Ning, Z. Tang, P. Xie, J. Hu, and Z. Fu, "Study on Silicone Rubber Composite Insulator Modified by High-Energy Electron Beam Irradiation," *IEEE Trans. Dielectr. Electr. Insul.*, vol. 30, no. 1, pp. 31–40, Feb. 2023, doi: 10.1109/TDEI.2022.3219374.

[19] J. Boden, C. R. Bowen, A. Buchard, M. G. Davidson, and C. Norris, "Understanding the Effects of Cross-Linking Density on the Self-Healing Performance of Epoxidized Natural Rubber and Natural Rubber," *ACS Omega*, vol. 7, no. 17, pp. 15098–15105, May 2022, doi: 10.1021/acsomega.2c00971.

[20] B. X. Du, Z. L. Ma, Y. Gao, and T. Han, "Effect of ambient temperature on electrical treeing characteristics in silicone rubber," *IEEE Trans. Dielectr. Electr. Insul.*, vol. 18, no. 2, pp. 401–407, Apr. 2011, doi: 10.1109/TDEI.2011.5739443.

[21] C. Xu, D. Wu, Q. Lv, and L. Yan, "Crystallization Temperature as the Probe to Detect Polymer-Filler Compatibility in the Poly(ε-caprolactone) Composites with Acetylated Cellulose Nanocrystal," *J. Phys. Chem. C*, vol. 121, no. 34, pp. 18615–18624, Aug. 2017, doi: 10.1021/acs.jpcc.7b05055.

[22] G. Kraus, "Interactions of Elastomers and Reinforcing Fillers," *Rubber Chem. Techn.*, vol. 38, no. 5, pp. 1070–1114, Nov. 1965, doi: 10.5254/1.3547105.

[23] V. Kumar, R. R. Wu, and D. J. Lee, "Morphological aspects of carbon nanofillers and their hybrids for actuators and sensors," *Polym. Compos.*, vol. 40, pp. E373–E382, Jan. 2019, doi: 10.1002/pc.24692.

[24] S. Banerjee, S. Saini, and S. Prasad D, "Electrical discharge resistance of polymeric nanocomposites," *IET Nanodielectrics*, vol. 4, no. 4, pp. 210–222, Dec. 2021, doi: 10.1049/nde2.12019.

[25] Y. Zhang, H. Wang, Z. Huang, and J. Li, "Enhanced surface flashover performance of oriented hexagonal boron nitride composites via anisotropic charge transportation," *High Volt.*, Art. no. hve2.12411, Jan. 2024, doi: 10.1049/hve2.12411.

[26] H. H. Horowitz and G. Metzger, "A New Analysis of Thermogravimetric Traces," *Anal. Chem.*, vol. 35, no. 10, pp. 1464–1468, Sep. 1963, doi: 10.1021/ac60203a013.

[27] J. Manoj Dhivakar, S. Kornhuber, and R. Sarathi, "Enhanced Mechanical, Thermal, and Erosion Resistance Properties via the Synergetic Effect of n-ATH/LMGP Added Ceramifiable Silicone Rubber Composites for Electrical Insulation," *Silicon*, vol. 16, no. 5,

pp. 1917-1928, Apr. 2024, doi: 10.1007/s12633-023-02802-y

[28] S. Ziraki, S. M. Zebarjad, and M. J. Hadianfard, "A study on the tensile properties of silicone rubber/polypropylene fibers/silica hybrid nanocomposites," *J. Mech. Behav. Biomed. Mater.*, vol. 57, pp. 289–296, Apr. 2016, doi: 10.1016/j.jmbbm.2016.01.019.

[29] B. Pukanszky and G. VÖRÖS, "Mechanism of interfacial interactions in particulate filled composites," *Compos. Interfaces*, vol. 1, no. 5, pp. 411–427, Jan. 1993, doi: 10.1163/156855493x00266.